



LIQUID LEVEL TRACKING FOR A COUPLED TANK SYSTEM USING QUASI-LPV CONTROL

SEGUIMIENTO DEL NIVEL DE LÍQUIDO DE UN SISTEMA DE TANQUES ACOPLADO EMPLEANDO CONTROL CUASI-LPV

Pedro Teppa-Garrán^{1,*} , Diego Muñoz-de Escalona¹ ,
 Javier Zambrano¹ 

Received: 13-03-2024, Received after review: 21-05-2024, Accepted: 03-07-2024, Published: 01-01-2025

Abstract

This article proposes a gain-scheduling procedure based on quasi-LPV modeling for a nonlinear coupled tank system to track the liquid level with zero steady-state error. The nonlinearities are directly represented by a parameter vector that varies within a bounded set constrained by the physical limits of the tank system levels. This approach enables accurate nonlinear system modeling using a linear parameter-varying model. State-feedback linear controllers are designed at the extreme vertices of the bounded set. The global controller is derived as the weighted average of local controller contributions, with the weighting determined by the instantaneous values of the parameter vector. Two interpolation mechanisms are proposed to implement this weighted averaging of the linear controllers. The results confirm the effectiveness of the proposed method in achieving accurate liquid level tracking.

Keywords: Coupled-Tank System, Gain Scheduling, Nonlinear Systems, Quasi-LPV, Tracking Problem

Resumen

En este artículo se propone un procedimiento de programación de ganancias basado en un modelado cuasi-LPV de un sistema no lineal de tanques acoplados para seguir el nivel de líquido con error en estado estacionario nulo. Las no linealidades están representadas directamente por un vector de parámetros que varía dentro de un conjunto acotado por los límites físicos del nivel del sistema de tanques. Esto permite un modelado exacto del sistema no lineal utilizando un modelo lineal de parámetros variantes. Luego, se diseñan controladores lineales de realimentación de estado en los vértices extremos del conjunto acotado. El controlador global corresponde a un promedio ponderado de las contribuciones locales. Esta ponderación depende de los valores instantáneos del vector de parámetros. Para implementar el promedio ponderado de los controladores lineales, se proponen dos mecanismos de interpolación. Los resultados obtenidos muestran la efectividad del método.

Palabras clave: sistema de tanques acoplados, programación de ganancias, sistemas no lineales, cuasi-LPV, problema de seguimiento

^{1,*}Departamento de Gestión de Proyectos y Sistemas, Universidad Metropolitana, Caracas, Venezuela.
 Corresponding author ✉: pteppa@unimet.edu.ve.

Suggested citation: Teppa-Garrán, P.; Muñoz-de Escalona, D. and Zambrano, J. "Liquid level tracking for a coupled tank system using quasi-lpv control," *Ingenius, Revista de Ciencia y Tecnología*, N.º 33, pp. 15-26, 2025, DOI: <https://doi.org/10.17163/ings.n33.2025.02>.

1. Introduction

The control of liquid levels in tanks is widely employed in various industries, including food and beverage production, nuclear and petrochemical plants, and the pharmaceutical sector. Generally, interactions between tanks occur due to coupling, resulting in nonlinear behavior [1]. Numerous control strategies have been proposed for coupled tank systems, including Proportional-Integral-Derivative (PID) controllers [2–4], Fuzzy control [5,6], Model Predictive Control [7,8], Backstepping Control [9,10], Sliding-Mode Control [11,12], Fractional PID controllers [13,14], Robust control [15]. Active Disturbance Rejection Control [16,17] and Two-Degree-Of-Freedom controllers [18]. Some of these techniques rely on nonlinear system theory, which can be challenging to implement, while others employ linearization of the system equations around an operating point. For the local operating range, designs based on Jacobian linearization perform effectively. However, under significant disturbances or when faster settling times are required, the performance of such controllers can deteriorate due to a loss of robustness.

Gain scheduling [19,20] is a widely adopted approach in industry for controlling nonlinear systems by breaking down the nonlinear design problem into several smaller, manageable subproblems where linear design tools can be applied. For instance, in robot control, controller dynamics are adjusted in real-time based on varying inertia and geometry. Similarly, most aircraft control laws are modified by interpolating individually designed controllers. In recent decades, the Linear Parameter Varying (LPV) system theory has gained prominence as a powerful paradigm for system identification, analysis, and controller synthesis [21–23]. This class of systems is particularly valuable as it allows nonlinearities to be incorporated as varying parameters within a bounded set, ensuring that the possible trajectories of the LPV system encompass all trajectories of the original nonlinear system. When these parameters include state vector elements, the system is referred to as quasi-LPV [24]. In this study, the nonlinearities of the tank system model, represented by liquid levels, are considered uncertain but constrained within the technological limits of the equipment ($[0, 30]cm$). This allows for an accurate representation of the nonlinear terms by embedding them into a quasi-LPV model. The advantage of this approach is that it enables the design of linear controllers using state-space techniques, ensuring zero steady-state tracking error for constant reference inputs and guaranteeing a pole-dominant criterion [25,26].

Within a gain-scheduling scheme, the control of the nonlinear coupled tank system is achieved through local controller interpolation. Two interpolation mechanisms are proposed: (1) analytical interpolation, where a system of linear equations is continuously solved to

compute the weighting factors, and (2) geometric interpolation, where the weights of the local controllers are determined based on the Euclidean distance to some vertex points. Analytical interpolation, initially presented in [27] and inspired by concepts from Takagi-Sugeno fuzzy models, is implemented in this study in a simplified form without incorporating any fuzzy elements. Geometric interpolation, on the other hand, offers an innovative approach in this context. While quasi-LPV theory has been widely applied in fields such as missile guidance [28,29] and robotics [30,31], its application to tank systems remains relatively unexplored despite the significant industrial relevance of this process.

The results confirm the effectiveness of the proposed method in controlling the coupled tank system. The article is structured as follows: Section 2 details the quasi-LPV control design method, with a particular focus on the formulation of two interpolation mechanisms, which are integrated within a gain-scheduled tracking control strategy and describes the coupled tank system's nonlinear model. In Section 3, the quasi-LPV design method is applied to the system. Finally, the conclusions are presented in Section 4.

Notación: Bold capital letters denote matrices, while bold lowercase letters represent vectors (i.e. θ_j is the j -th component of the vector $\boldsymbol{\theta}$). Superscripts indicate vectors; for instance, $\boldsymbol{\theta}^i$ refers to the i -th vector, and θ_j^i denotes the j -th component of the i -th vector. $\dot{f}(t) = df(t)/dt$ and $\ddot{f}(t) = d^2f(t)/dt^2$. \mathbb{R} denotes the set of real numbers.

2. Materials and methods

2.1. Quasi-LPV control design

Most existing nonlinear controller synthesis approaches focus on input-affine systems [32], which are typically described as equation (1):

$$\dot{\mathbf{x}}(t) = \mathbf{f}[\mathbf{x}(t)] + \mathbf{g}[\mathbf{x}(t)]u(t) \quad (1)$$

Where $\mathbf{x} : \mathbb{R}_+ \rightarrow \mathbb{R}^n$ is the state vector, $u : \mathbb{R}_+ \rightarrow \mathbb{R}$ is the control input, t is the independent variable of time, $\mathbf{f} : \mathbb{R}^n \rightarrow \mathbb{R}^n$ and $\mathbf{g} : \mathbb{R}^n \rightarrow \mathbb{R}^n$ are nonlinear fields. The general nonlinear equation $\dot{\mathbf{x}}(t) = \mathbf{f}[\mathbf{x}(t), u(t)]$, which frequently appears, can, under technical assumptions, be transformed into (1) through a nonlinear feedback transformation [33].

The first step in the synthesis procedure is to derive a quasi-LPV representation of the form as seen in the equation (2):

$$\dot{\mathbf{x}}(t) = \mathbf{A}[\boldsymbol{\theta}(t)]\mathbf{x}(t) + \mathbf{B}[\boldsymbol{\theta}(t)]u(t), \boldsymbol{\theta} \in \Omega \quad (2)$$

For the nonlinear system described in equation (1). Here $\boldsymbol{\theta}$ represents a parameter vector that varies

within a bounding box Ω . In quasi-LPV modeling, it is assumed that there is a relationship between the parameter vector and the system states, $\boldsymbol{\theta} = \boldsymbol{\sigma}(\mathbf{x})$, such that for all parameter values within Ω .

$$\mathbf{A}[\boldsymbol{\theta}(t)]\mathbf{x}(t) + \mathbf{B}[\boldsymbol{\theta}(t)]u(t) = \mathbf{f}[\mathbf{x}(t)] + \mathbf{g}[\mathbf{x}(t)]u(t)$$

2.2. Interpolation mechanisms

Defining $\boldsymbol{\theta}^i \in \mathbb{R}^n$, $i = 1, \dots, N$ in equation (2) as the vectors representing the extreme combinations of parameters in Ω , a set of local linearized models is obtained as follows:

$$(\mathbf{A}_i, \mathbf{B}_i) = (\mathbf{A}(\boldsymbol{\theta}^i), \mathbf{B}(\boldsymbol{\theta}^i)), i = 1, \dots, N \quad (3)$$

For each local model, a state vector gain \mathbf{K}_i can be designed. The parameter vector $\boldsymbol{\theta}(t)$ is then used to construct the overall gain-scheduled controller by interpolating the local controllers. At any given time, $\boldsymbol{\theta}(t)$ can be expressed as equation (4):

$$\boldsymbol{\theta}(t) = \sum_{i=1}^N \alpha_i(t) \boldsymbol{\theta}^i, \sum_{i=1}^N \alpha_i(t) = 1 \quad (4)$$

The weights $\alpha_i(t)$ are computed by solving the system of linear equations:

$$\mathbf{W}\boldsymbol{\eta} = \mathbf{v} \quad (5)$$

Where:

$$\boldsymbol{\eta} = \begin{bmatrix} \alpha_1(t) \\ \vdots \\ \alpha_N(t) \end{bmatrix}, \quad \mathbf{W} = \begin{bmatrix} \boldsymbol{\theta}^1 & \dots & \boldsymbol{\theta}^N \\ 1 & \dots & 1 \end{bmatrix}, \quad \mathbf{v} = \begin{bmatrix} \boldsymbol{\theta}(t) \\ 1 \end{bmatrix}$$

The interpolation scheme based on the weights computed from the continuous solution of equation (5) is referred to as analytical interpolation to distinguish it from geometric interpolation, which will be described below.

At any given time, the Euclidean distance between the state-dependent parameter vector $\boldsymbol{\theta} \in \mathbb{R}^n$ and any of the extreme vectors $\boldsymbol{\theta}^i \in \mathbb{R}^n$ within the bounding box Ω can be computed for $i = 1, \dots, N$ as:

$$\overline{\boldsymbol{\theta}\boldsymbol{\theta}^i} = \sqrt{(\theta_1 - \theta_1^i)^2 + \dots + (\theta_n - \theta_n^i)^2} \quad (6)$$

The relative contribution of the parameter vector $\boldsymbol{\theta}(t)$ on each vertex $\boldsymbol{\theta}^i$ is given by:

$$a_j = \frac{\overline{\boldsymbol{\theta}\boldsymbol{\theta}^j}}{\sum_i \overline{\boldsymbol{\theta}\boldsymbol{\theta}^i}}, j = 1, \dots, N$$

Points further from the vertices should have lower weights. Therefore, the complementary distance, $1 -$

$\overline{\boldsymbol{\theta}\boldsymbol{\theta}^i}$, is used in the calculation. The complementary relative contribution is then computed as $b_j = 1 - a_j$, $j = 1, \dots, N$. Finally, the weight $\alpha_j(t)$ para $j = 1, \dots, N$ at any given time is determined as:

$$\alpha_j = \frac{b_j}{\sum_{i=1}^N b_i} = \frac{1 - \frac{\overline{\boldsymbol{\theta}\boldsymbol{\theta}^j}}{\sum_{i=1}^N \overline{\boldsymbol{\theta}\boldsymbol{\theta}^i}}}{\sum_{j=1}^N \left(1 - \frac{\overline{\boldsymbol{\theta}\boldsymbol{\theta}^j}}{\sum_{i=1}^N \overline{\boldsymbol{\theta}\boldsymbol{\theta}^i}}\right)} \quad (7)$$

As in the analytical procedure, the weights computed using the geometric approach continuously satisfy the equation $\sum_{j=1}^N \alpha_j(t) = 1$. The key difference between the two methods is that the geometric approach ensures positive weights, whereas the analytical procedure does not. This may necessitate conditioning of the control input if the actuator operates only with positive signals.

2.3. Tracking a step reference input

Using the computed weights, the model in equation (2) can be approximated as a combination of the local linear models:

$$\dot{\mathbf{x}}(t) = \underbrace{\sum_{i=1}^N \alpha_i(t) \mathbf{A}_i}_{\mathbf{A}} \mathbf{x}(t) + \underbrace{\sum_{i=1}^N \alpha_i(t) \mathbf{B}_i}_{\mathbf{B}} \mathbf{u}(t) \quad (8)$$

The design problem now focuses on tracking a step reference input $r(t)$ with zero steady-state error $e(t)$ defined as:

$$e(t) = r(t) - y(t) \quad (9)$$

Where is the controlled output. Taking the time derivative of equation (9), for a constant reference input yields:

$$y(t) = \mathbf{C}\mathbf{x}(t) \quad (10)$$

$$\dot{e}(t) = -\mathbf{C}\dot{\mathbf{x}}(t) \quad (11)$$

Taking the time derivative of each local linear model $(\mathbf{A}_i, \mathbf{B}_i)$ for $i = 1, \dots, N$ yields:

$$\dot{\mathbf{x}}(t) = \mathbf{A}_i \dot{\mathbf{x}}(t) + \mathbf{B}_i \dot{\mathbf{u}}(t) \quad (12)$$

Equations (11) and (12) can be combined as:

$$\dot{\mathbf{z}}(t) = \mathbf{F}_i \mathbf{z}(t) + \mathbf{G}_i u_0(t) \quad (13)$$

Where:

$$\mathbf{z}(t) = [e(t) \quad \dot{\mathbf{x}}(t)]^T, \quad u_0(t) = \dot{\mathbf{u}}(t),$$

$$\mathbf{F}_i = \begin{bmatrix} 0 & -\mathbf{C} \\ \mathbf{0} & \mathbf{A}_i \end{bmatrix}, \quad \mathbf{G}_i = \begin{bmatrix} 0 \\ \mathbf{B}_i \end{bmatrix}.$$

A state feedback gain for system (13) is constructed as:

$$u_0(t) = \mathbf{K}_i \mathbf{z}(t) = \begin{bmatrix} K_{e_i} & \mathbf{K}_{x_i} \end{bmatrix} \begin{bmatrix} e(t) \\ \dot{\mathbf{x}}(t) \end{bmatrix} \quad (14)$$

After integrating equation (14), the actual control signal becomes:

$$u(t) = K_{e_i} \int_0^t e(\tau) d\tau + \mathbf{K}_{x_i} \mathbf{x}(t) \quad (15)$$

Using the same weights $\alpha_i(t)$, a time-varying state feedback gain for system (8) is constructed as:

$$u(t) = \tilde{K}_e \int_0^t e(\tau) d\tau + \tilde{\mathbf{K}}_x \mathbf{x}(t) \quad (16)$$

Where:

$$\tilde{K}_e(t) = \sum_{i=1}^N \alpha_i(t) K_{e_i}, \quad \tilde{\mathbf{K}}_x(t) = \sum_{i=1}^N \alpha_i(t) \mathbf{K}_{x_i}$$

Figure 1 illustrates the implementation of the control policy described in equation (15) for each local model, as defined in equation (3). Additionally, Figure 2 depicts the global controller that enables the implementation of the control law in equation (16) by interpolating the local controllers, either using weights computed analytically (equation (5)) or geometrically (equation (7)). For the augmented tracking system in equation (13), the gain $\mathbf{K}_i = \begin{bmatrix} \underbrace{K_{e_i}}_{(1 \times 1)} & \underbrace{\mathbf{K}_{x_i}}_{(1 \times N)} \end{bmatrix}$ is computed for each $i = 1, \dots, N$ by solving a closed-loop pole placement problem using the Matlab command:

$$\gg \mathbf{K}_i = \text{place}(\mathbf{F}_i, \mathbf{G}_i, P) \quad (17)$$

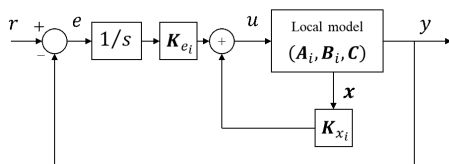


Figure 1. Local tracking control system block diagram

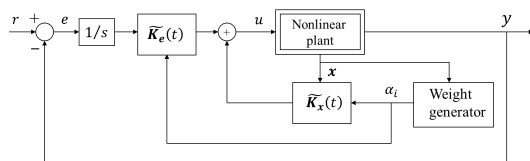


Figure 2. Overall tracking controller implementation by interpolating local controllers

Where P represents the desired closed-loop poles, selected to satisfy a guaranteed pole-dominant criterion [25, 26], based on closed-loop design requirements specified in the time domain, such as overshoot (OS) and settling time (T_s). In light of the above discussion, the design algorithm for implementing the interpolated control law in equation (16) is summarized in Table 1.

Table 1. Design algorithm for quasi-LPV control

Step 1	Construct a quasi-LPV model (2) for the nonlinear system to be controlled (1).
Step 2	From (2), derive a set of local linearized models (3).
Step 3	Compute the local gains k_{e_i} y \mathbf{K}_{x_i} en (15) para cada modelo de seguimiento local aumentado en (13), in (15) for each local tracking augmented model in (13), using the closed-loop specifications for OS y T_s through the Matlab command (17).
Step 4	Compute the weights α_i by continuously solving (5) or (7).
Step 5	Interpolate the local controllers obtained in Step (2) through (16).

2.4. Coupled Tank System

Figure 3 depicts the coupled tank system. It consists of a single pump and two tanks, each equipped with a pressure sensor to measure the water level. The pump transfers water from the bottom reservoir to the top of the system. Depending on the configuration of the outflow valves, water can flow into the upper tank, the lower tank, or both. This configuration is illustrated in Figure 4, where the pump output is connected to the first tank.

x_1 and x_2 represent the water levels in tanks 1 and 2, respectively. The vector functions in the form of equation (18) for the coupled tank system are derived using Bernoulli's law and the mass balance principle [34] and are expressed as:

$$\mathbf{f}(\mathbf{x}) = \begin{bmatrix} -(Ad_1/A_1 \sqrt{2gx_1(t)}) & 0 \\ (Ad_1/A_2 \sqrt{2gx_1(t)}) & -(Ad_2/A_2 \sqrt{2gx_2(t)}) \end{bmatrix} \\ \mathbf{g}(\mathbf{x}) = \begin{bmatrix} K_f/A_1 \\ 0 \end{bmatrix} \quad (18)$$



Figure 3. Coupled tank system

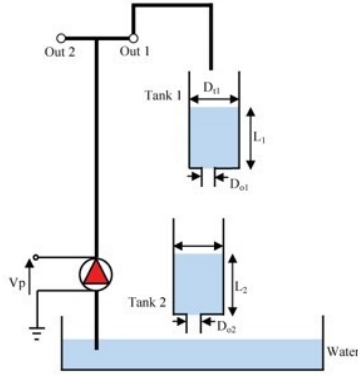


Figure 4. Standard configuration of the coupled tank system

Where A_1 and A_2 denote the cross-sectional areas of tanks 1 and 2, respectively. A_{d1}, A_{d2} represent the cross-sectional areas of the corresponding orifices, g is the acceleration on Earth due to gravity, and K_f is the pump flow constant. The numerical values of these parameters are provided in Table 2.

Table 2. Physical parameters of the coupled tank system

Description	Value	Unit
Pump flow constant (K_f)	4	$cm^3/s/V$
Small Outflow Orifice Diameter of Tank 1 (D_{o1})	0.635	cm
Small Outflow Orifice Diameter of Tank 2 (D_{o2})	0.476	cm
Tanks' Diameter (D_{t1}, D_{t2})	4.445	cm
Water levels range of Tanks 1 and 2	30	cm
Acceleration due to gravity (g)	981	cm/s^2
Pump peak voltage	22	V

3. Results and discussion

This section outlines the implementation and evaluates the performance of the quasi-LPV control method, as summarized in Table 1.

3.1. Quasi-LPV model

The input voltage applied to the pump serves as the control signal, while the water level in the second tank is selected as the controlled output. Based on equation (18), the nonlinear model of the tank system can be expressed as:

$$\dot{x}_1(t) = -\frac{Ad_1}{A_1} \sqrt{2gx_1(t)} + \frac{K_f}{A_1} u(t)$$

$$\dot{x}_2(t) = \frac{Ad_1}{A_2} \sqrt{2gx_1(t)} - \frac{Ad_2}{A_2} \sqrt{2gx_2(t)}$$

The nonlinear terms in each equation can be reformulated as follows:

$$\dot{x}_1(t) = -\frac{Ad_1}{A_1} \sqrt{\frac{2gx_1^2(t)}{x_1(t)}} + \frac{K_f}{A_1} u(t)$$

$$\dot{x}_2(t) = \frac{Ad_1}{A_2} \sqrt{\frac{2gx_1^2(t)}{x_1(t)}} - \frac{Ad_2}{A_2} \sqrt{\frac{2gx_2^2(t)}{x_2(t)}}$$

Resulting in:

$$\dot{x}_1(t) = -\frac{Ad_1\sqrt{2g}}{A_1} \sqrt{\frac{1}{x_1(t)}} x_1(t) + \frac{K_f}{A_1} u(t) \quad (19)$$

$$\dot{x}_2(t) = \frac{Ad_1\sqrt{2g}}{A_2} \sqrt{\frac{1}{x_1(t)}} x_1(t) - \frac{Ad_2\sqrt{2g}}{A_2} \sqrt{\frac{1}{x_2(t)}} x_2(t)$$

Defining the parameter vector in (19) as:

$$\theta(t) = [\theta_1(t) \ \theta_2(t)]^T = [1/\sqrt{x_1} \ 1/\sqrt{x_2}]^T \quad (20)$$

Utilizing the numerical values from Table 2, the quasi-LPV model in the form of equation (2) is expressed as:

$$\dot{\mathbf{x}}(t) = \begin{bmatrix} -0.904\theta_1(t) & 0 \\ 0.904\theta_1(t) & -0.508\theta_2(t) \end{bmatrix} \mathbf{x}(t) + \begin{bmatrix} 0.258 \\ 0 \end{bmatrix} u(t) \quad (21)$$

$$y(t) = \underbrace{[0 \ 1]}_C \mathbf{x}(t)$$

The liquid levels in the tanks are considered uncertain but vary within their physical limits, as specified in Table 2, over the interval:

$$x_1(t), x_2(t) \in [5 \ 25] cm \quad (22)$$

When the liquid levels in the tanks vary within the range specified in equation (22), the parameter vector in equation (20) will fluctuate within the rectangular bounding box:

$$\theta_1(t), \theta_2(t) \in [0.20 \ 0.45] \quad (23)$$

3.2. Local linearized models

The extreme parameter combinations within the bounding box in equation (23) yield the following vectors:

$$\begin{aligned} \theta^1 &= \begin{bmatrix} 0.20 \\ 0.20 \end{bmatrix}, & \theta^2 &= \begin{bmatrix} 0.20 \\ 0.45 \end{bmatrix}, \\ \theta^3 &= \begin{bmatrix} 0.45 \\ 0.20 \end{bmatrix}, & \theta^4 &= \begin{bmatrix} 0.45 \\ 0.45 \end{bmatrix} \end{aligned} \quad (24)$$

This results in the following set of local linearized models: $(\mathbf{A}_i, \mathbf{B}_i) = (\mathbf{A}(\theta^i), \mathbf{B})$ for $i = 1, \dots, 4$.

$$\begin{aligned} \mathbf{A}_1 &= \begin{bmatrix} -0.181 & 0 \\ 0.181 & -0.102 \end{bmatrix} & \mathbf{A}_2 &= \begin{bmatrix} -0.181 & 0 \\ 0.181 & -0.229 \end{bmatrix} \\ \mathbf{A}_3 &= \begin{bmatrix} -0.407 & 0 \\ 0.407 & -0.102 \end{bmatrix} & \mathbf{A}_4 &= \begin{bmatrix} -0.407 & 0 \\ 0.407 & -0.229 \end{bmatrix} \\ \mathbf{B} &= \begin{bmatrix} 0.258 \\ 0 \end{bmatrix} \end{aligned} \quad (25)$$

3.3. Local controllers

Using equation (25), the augmented systems in equation (13) for each vertex are given by:

$$\dot{z}(t) = \begin{bmatrix} 0 & -\mathbf{C} \\ \mathbf{0} & \mathbf{A}_i \end{bmatrix} z(t) + \begin{bmatrix} 0 \\ \mathbf{B} \end{bmatrix} u_0(t) \quad (26)$$

The four controller gains \mathbf{K}_i in equation (15) are computed using the closed-loop time domain specifications $OS = 1\%$ and $T_s = 40s$. The calculation is then performed as outlined in [35].

$$\begin{aligned} OS &= e^{(-\zeta\pi/\sqrt{1-\zeta^2})} \Rightarrow \zeta = \frac{1}{\sqrt{1 + \left(\frac{\pi}{\ln(OS)}\right)^2}} \\ &= 0.83 \\ T_s &= 4/\zeta\omega_n \Rightarrow \omega_n = \frac{4}{\zeta T_s} = 0.1 \end{aligned}$$

The resulting dominant poles $p_{1,2} = -0.0996 \pm j0.0669(s^2 + 0.1992s + 0.0144)$. The desired closed-loop poles used in equation (17) are $P = [-0.0996 \pm j0.0669, -0.996]$, where $p_3 = -0.996$ is a fast pole with negligible influence on the OS and T_s specifications. The controller gains are computed using equation (17) as follows:

$$\begin{aligned} \mathbf{K}_1 &= \left[\begin{array}{c|cc} \underbrace{-0.3161}_{K_{e_1}} & \underbrace{3.5380 \quad 2.1888}_{K_{x_1}} \\ \hline \underbrace{-0.3161}_{K_{e_2}} & \underbrace{3.0457 \quad -0.1663}_{K_{x_2}} \\ \hline \underbrace{-0.1405}_{K_{e_3}} & \underbrace{2.6620 \quad 0.9728}_{K_{x_3}} \\ \hline \underbrace{-0.1405}_{K_{e_4}} & \underbrace{2.1698 \quad -0.0739}_{K_{x_4}} \end{array} \right] \end{aligned} \quad (27)$$

3.4. Interpolation mechanisms

In the analytical approach, equation (5) is represented as the following system of linear equations:

$$\underbrace{\begin{bmatrix} 0.20 & 0.20 & 0.45 & 0.45 \\ 0.20 & 0.45 & 0.20 & 0.45 \\ 1 & 1 & 1 & 1 \end{bmatrix}}_W \begin{bmatrix} \alpha_1(t) \\ \alpha_2(t) \\ \alpha_3(t) \\ \alpha_4(t) \end{bmatrix} = \begin{bmatrix} \theta_1(t) \\ \theta_2(t) \\ 1 \end{bmatrix}$$

Solving this system using the pseudoinverse matrix $(\mathbf{W}^T \mathbf{W})^{-1} \mathbf{W}^T$ yields the following equation:

$$\begin{bmatrix} \alpha_1(t) \\ \alpha_2(t) \\ \alpha_3(t) \\ \alpha_4(t) \end{bmatrix} = \begin{bmatrix} -0.50 & -0.50 & 1 \\ -3.25 & 0.75 & 1 \\ 0.75 & -3.25 & 1 \\ 3.50 & 3.50 & -2 \end{bmatrix} \begin{bmatrix} \theta_1(t) \\ \theta_2(t) \\ 1 \end{bmatrix} \quad (28)$$

For geometric interpolation, equation (7) is implemented directly using a Matlab function block. A straightforward Matlab function code is written and integrated into a Simulink model, which executes the simulation.

3.5. Gain-scheduled control implementation

The gain-scheduled control strategy depicted in Figure 2 was implemented. Figure 5 illustrates the liquid level response in the second tank following a set-point change, comparing both interpolation methods for the computed linear controllers (27).

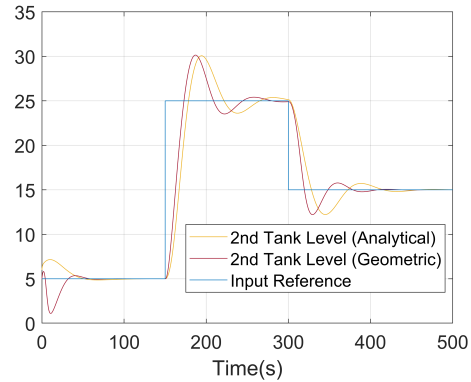


Figure 5. Second tank closed-loop liquid level response for analytical and geometric interpolation methods

The geometric method encounters specific issues at the start of the simulation due to its inability to provide the required negative control action. After this initial phase, the performance of both interpolation schemes becomes comparable.

Figure 6 illustrates the control signal, while Figure 7 focuses on the first 20 seconds of the control signal.

It is evident that when a negative control signal is required, the geometric scheme remains at zero, confirming the issues observed at the beginning of the simulation, as depicted in Figure 5. It is important to note that the control signal provided by the pump cannot be negative, a limitation not accounted for during the simulation when evaluating the performance of both interpolation schemes.

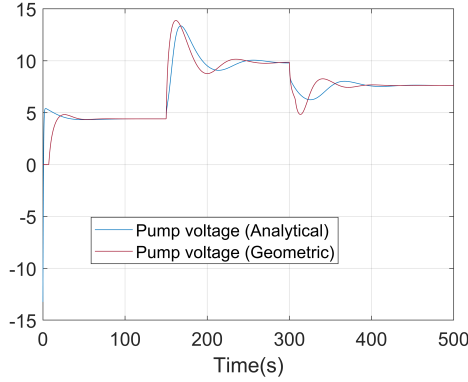


Figure 6. Pump voltage control signal for analytical and geometric interpolation methods

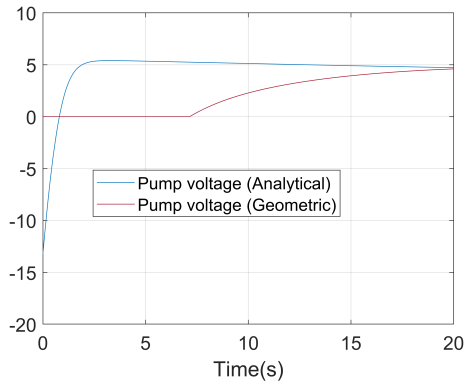


Figure 7. Detail of the control signal during the first 20 s

3.6. Further results

Figure 8 illustrates the parametric bounding box defined by equation (23). The previous results involved the implementation of the gain scheduled controller through the interpolation both geometric and analytical of the local controllers computed at the vertices (A), (B), (C), and (D), based on a dominant pole criterion for the desired OS and T_s specifications. Additionally, the simulation permitted the control signal to take on negative values to facilitate a comparison between the two interpolation mechanisms.

The gain-scheduled controller is implemented in this section, using various local controllers computed within the region shown in Figure 8, as specified in

Table 3. The control signal is constrained to remain within the operational range of the pump (0-22 V), and the desired closed-loop poles in equation (17) are selected as $P = [-0.1, -0.2, -10]$, rather than employing the dominant pole criterion.

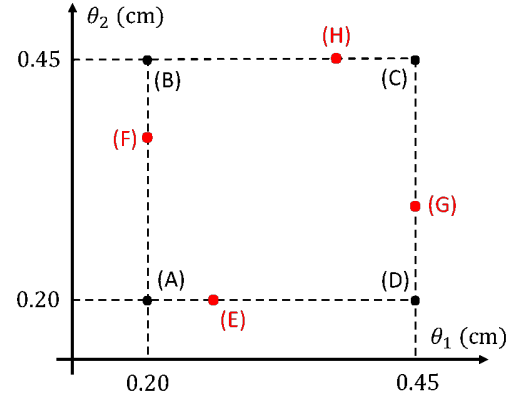


Figure 8. Points chosen in the parametric bounding box (23) to compute local controllers

Table 3. Points chosen in region (3) to compute local controllers.

Model	Points chosen in (23)
M1	(A), (B), (C), (D)
M2	(E), (F), (G), (H)
M3	(A), (D)

Model M1 utilizes the vertices of the region, M2 computes the local controllers along the edges, and model M3 considers the extreme vertices of the region, where parameters θ_1 and θ_2 take their minimum and maximum possible values. The selection of the M3 model is justified by the well-known Edge Theorem [36]. Figure 9 illustrates the level in the second tank and the pump control signal using the M1 model with analytical interpolation.

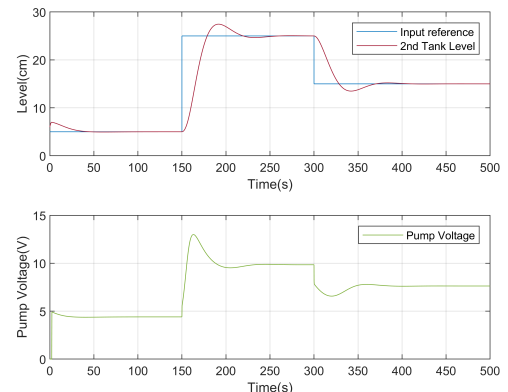


Figure 9. Second tank level and pump voltage for M1 model and analytical interpolation

Figure 10 presents a similar scenario employing geometric interpolation. Figures 11, 12 replicate the analysis for the M2 model, using analytical and geometric interpolation mechanisms, respectively.

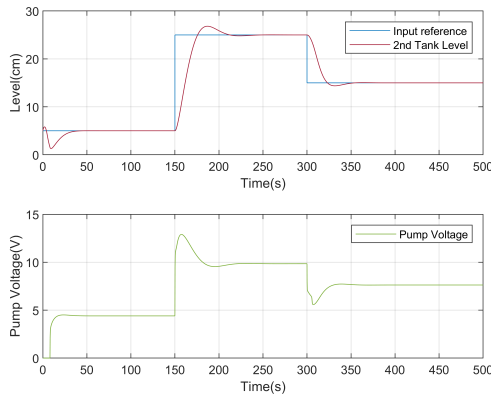


Figure 10. Second tank level and pump voltage for M1 model and geometric interpolation

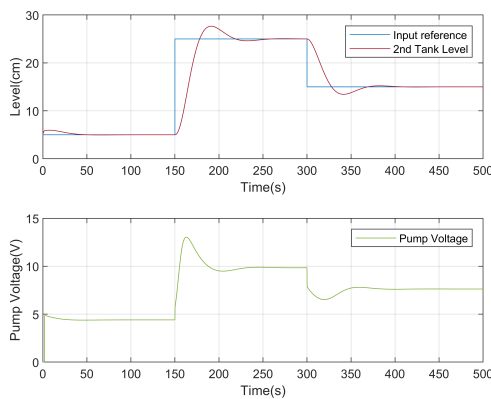


Figure 11. Second tank level and pump voltage for M2 model and analytical interpolation

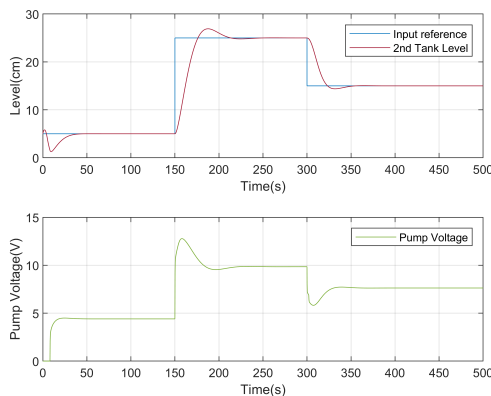


Figure 12. Second tank level and pump voltage for M2 model and geometric interpolation

Figures 13 and 14 display the results for the M3 model, again using analytical and geometric interpolation, respectively. Finally, Figures 15 and 16 compare the evolution of the liquid level in the second tank for all three models, with analytical and geometric interpolation considered, respectively.

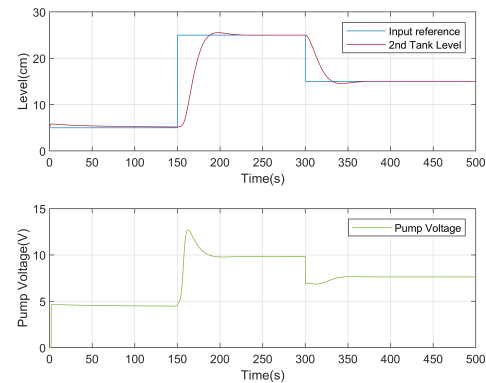


Figure 13. Second tank level and pump voltage for M3 model and analytical interpolation

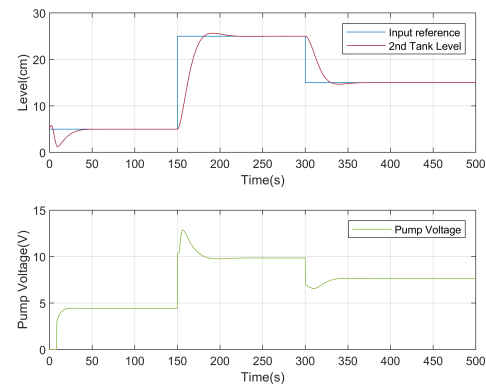


Figure 14. Second tank level and pump voltage for M3 model and geometric interpolation

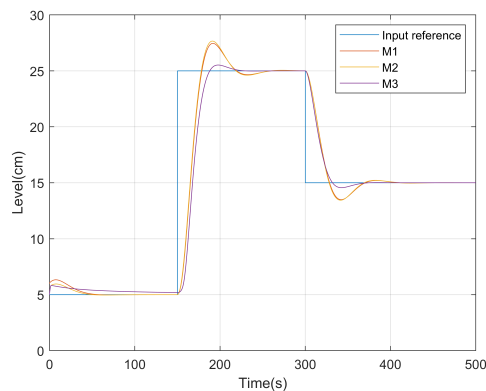


Figure 15. Second tank level for models M1, M2 and M3 using analytical interpolation

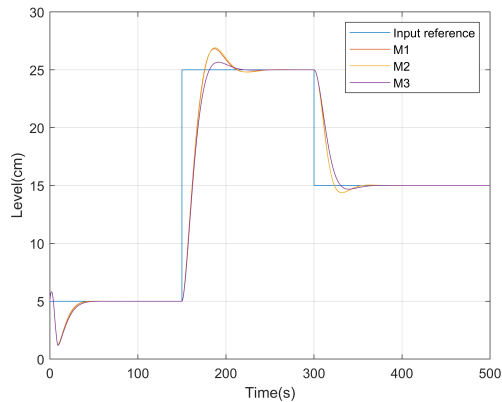


Figure 16. Second tank level for models M1, M2 and M3 using geometric interpolation

4. Conclusions

A gain-scheduled procedure was proposed to control a coupled tank system modeled as a quasi-LPV system. The nonlinearities of the model are directly captured by a set of uncertain parameters that vary within a bounded set, constrained by the physical limits of the tank system. Extreme combinations of the parameter vector were computed, and local linear approximations were obtained. These approximations were then used in the state-space synthesis of control laws to track a constant reference input. The global controller was constructed as a weighted average of the local contributions, where the weights depended on the instantaneous values of the parameter vector. Two interpolation mechanisms, geometric and analytical, were employed to determine the weighted average of the linear controllers. The geometric method is based on the Euclidean distance between the parameter vector and the vertices, while the analytical method involves solving a linear system of equations using the pseudoinverse of a matrix. The geometric scheme is simpler and generates only positive control actions, with a very short computation time. In contrast, the analytical scheme can provide both positive and negative control actions but requires significantly more processing time. Simulation results demonstrated that using the two extreme vertices (Model M3) to compute the interpolated local controllers reduces the computational effort needed.

The primary limitation of the methodology is the challenge of accurately determining the quasi-LPV model to capture the system's nonlinearities, which is not an easy task for all plants. This indicates that the proposed approach may not be universally applicable. However, when a nonlinear plant can be effectively modeled using a linear parameter-varying system, the method is straightforward to implement and yields satisfactory results. Another key aspect

of the method is that the control law for designing the local controllers is not limited to closed-loop pole assignment, as demonstrated in this article. Various state-feedback control strategies can be employed, including those that account for optimality, robustness, and constraints. Additionally, although the guaranteed pole-dominant criterion is suitable for linear systems, a notable discrepancy emerged between the design specifications and the actual performance in the case of the nonlinear tank system. This gap was mitigated by setting dominant real poles to improve control over the output.

Ongoing work focuses on the real-time implementation of the proposed design method and the inclusion of state observers.

Acknowledgements

The authors gratefully acknowledge the support provided by the Research Program of the Metropolitan University in Caracas, Venezuela, under project number PG-A-13-21-22.

References

- [1] R. Grygiel, R. Bieda, and M. Blachuta, "On significance of second-order dynamics for coupled tanks systems," in *2016 21st International Conference on Methods and Models in Automation and Robotics (MMAR)*, 2016, pp. 1016–1021. [Online]. Available: <https://doi.org/10.1109/MMAR.2016.7575277>
- [2] S. K. Singh, N. Katal, and S. G. Modani, "Multi-objective optimization of pid controller for coupled-tank liquid-level control system using genetic algorithm," in *Proceedings of the Second International Conference on Soft Computing for Problem Solving (SocProS 2012), December 28-30, 2012*, B. V. Babu, A. Nagar, K. Deep, M. Pant, J. C. Bansal, K. Ray, and U. Gupta, Eds. New Delhi: Springer India, 2014, pp. 59–66. [Online]. Available: https://doi.org/10.1007/978-81-322-1602-5_7
- [3] D. L. Mute, S. R. Mahapatro, and K. K. Chaudhari, "Internal model based pi controller design for the coupled tank system: An experimental study," in *2016 IEEE First International Conference on Control, Measurement and Instrumentation (CMI)*, 2016, pp. 72–76. [Online]. Available: <https://doi.org/10.1109/CMI.2016.7413713>
- [4] M. G. Stohy, H. S. Abbas, A.-H. M. El-Sayed, and A. G. Abo El-maged, "Parameter estimation and pi control for a water coupled tank system," *Journal of Advanced Engineering Trends*, vol. 38,

- no. 2, pp. 147–159, 2020. [Online]. Available: <https://doi.org/10.21608/jaet.2020.73062>
- [5] L. Liang, “The application of fuzzy pid controller in coupled-tank liquid-level control system,” in *2011 International Conference on Electronics, Communications and Control (ICECC)*, 2011, pp. 2894–2897. [Online]. Available: <https://doi.org/10.1109/ICECC.2011.6067785>
- [6] A. Başçı and A. Derdiyok, “Implementation of an adaptive fuzzy compensator for coupled tank liquid level control system,” *Measurement*, vol. 91, pp. 12–18, 2016. [Online]. Available: <https://doi.org/10.1016/j.measurement.2016.05.026>
- [7] M. Essahafi, “Model predictive control (MPC) applied to coupled tank liquid level system,” *CoRR*, vol. abs/1404.1498, 2014. [Online]. Available: <https://doi.org/10.48550/arXiv.1404.1498>
- [8] J. Berberich, J. Köhler, M. A. Müller, and F. Allgöwer, “Data-driven model predictive control: closed-loop guarantees and experimental results,” *at - Automatisierungstechnik*, vol. 69, no. 7, pp. 608–618, Jun. 2021. [Online]. Available: <http://dx.doi.org/10.1515/auto-2021-0024>
- [9] J. Jiffy Anna, N. E. Jaffar, and F. Riya Mary, “Modelling and control of coupled tank liquid level system using backstepping method,” *International Journal of Engineering Research and Technology*, vol. 4, no. 6, pp. 667–671, 2015. [Online]. Available: <http://dx.doi.org/10.17577/IJERTV4IS060710>
- [10] J. Dai, B. Ren, and Q.-C. Zhong, “Uncertainty and disturbance estimator-based backstepping control for nonlinear systems with mismatched uncertainties and disturbances,” *Journal of Dynamic Systems, Measurement, and Control*, vol. 140, no. 12, Jul 2018, 121005. [Online]. Available: <https://doi.org/10.1115/1.4040590>
- [11] F. Abu Khadra and J. Abu Qudeiri, “Second order sliding mode control of the coupled tanks system,” *Mathematical Problems in Engineering*, vol. 2015, no. 1, p. 167852, 2015. [Online]. Available: <https://doi.org/10.1155/2015/167852>
- [12] K. K. Ayten and A. Dumlu, “Implementation of a pid type sliding-mode controller design based on fractional order calculus for industrial process system,” *Elektronika ir Elektrotechnika*, vol. 27, no. 6, pp. 4–10, Dec. 2021. [Online]. Available: <https://doi.org/10.5755/j02.eie.30306>
- [13] M. Vashishth, L. S. Rai, and A. V. R. Kumar, “Liquid level control of coupled tank system using fractional pid controller,” 2013. [Online]. Available: <https://upsalesiana.ec/ing33ar2r13>
- [14] P. Roy and B. Krishna Roy, “Fractional order pi control applied to level control in coupled two tank mimo system with experimental validation,” *Control Engineering Practice*, vol. 48, pp. 119–135, 2016. [Online]. Available: <https://doi.org/10.1016/j.conengprac.2016.01.002>
- [15] M. H. Jali, A. Ibrahim, R. Ghazali, C. C. Soon, and A. R. Muhammad, “Robust Control Approach of SISO Coupled Tank System,” *International Journal of Advanced Computer Science and Applications*, vol. 12, no. 1, 2021. [Online]. Available: <http://dx.doi.org/10.14569/IJACSA.2021.0120123>
- [16] P. Teppa, M. Bravo, and G. Garcia, “Control por rechazo activo de perturbaciones del nivel de líquido de un sistema de tanques acoplado,” *Revista Faraute de Ciencia y Tecnología*, vol. 7, no. 1, pp. 10–18, 2012. [Online]. Available: <https://upsalesiana.ec/ing33ar2r16>
- [17] P. Teppa Garran and G. Garcia, “Design of an optimal pid controller for a coupled tanks system employing adrc,” *IEEE Latin America Transactions*, vol. 15, no. 2, pp. 189–196, 2017. [Online]. Available: <https://doi.org/10.1109/TLA.2017.7854611>
- [18] P. Teppa Garran, M. Faggioni, and G. Garcia, “Optimal tracking in two-degree-of-freedom control systems: Coupled tank system,” *Journal of Applied Research and Technology*, vol. 21, no. 4, pp. 560–570, 2023. [Online]. Available: <https://doi.org/10.22201/icat.24486736e.2023.21.4.2000>
- [19] W. J. Rugh and J. S. Shamma, “Research on gain scheduling,” *Automatica*, vol. 36, no. 10, pp. 1401–1425, 2000. [Online]. Available: [https://doi.org/10.1016/S0005-1098\(00\)00058-3](https://doi.org/10.1016/S0005-1098(00)00058-3)
- [20] D. Rotondo, *Advances in Gain-Scheduling and Fault Tolerant Control Techniques*. Springer Cham, 2018. [Online]. Available: <https://doi.org/10.1007/978-3-319-62902-5>
- [21] G. S. X. Bombois, D. Ghosh and J. Huillery, “Lpv system identification for control using the local approach,” *International Journal of Control*, vol. 94, no. 2, pp. 390–410, 2021. [Online]. Available: <https://doi.org/10.1080/00207179.2019.1596316>
- [22] Z. GAO and J. FU, “Robust lpv modeling and control of aircraft flying through wind disturbance,” *Chinese Journal of Aeronautics*, vol. 32, no. 7, pp. 1588–1602, 2019. [Online]. Available: <https://doi.org/10.1016/j.cja.2019.03.029>

- [23] S. Li, A.-T. Nguyen, T.-M. Guerra, and A. Kruszewski, “Reduced-order model based dynamic tracking for soft manipulators: Data-driven lpv modeling, control design and experimental results,” *Control Engineering Practice*, vol. 138, p. 105618, 2023. [Online]. Available: <https://doi.org/10.1016/j.conengprac.2023.105618>
- [24] R. Robles, A. Sala, and M. Bernal, “Performance-oriented quasi-lpv modeling of nonlinear systems,” *International Journal of Robust and Nonlinear Control*, vol. 29, no. 5, pp. 1230–1248, 2019. [Online]. Available: <https://doi.org/10.1002/rnc.4444>
- [25] P. Persson and K. Astrom, “Dominant pole design - a unified view of pid controller tuning,” *IFAC Proceedings Volumes*, vol. 25, no. 14, pp. 377–382, 1992. [Online]. Available: [https://doi.org/10.1016/S1474-6670\(17\)50763-6](https://doi.org/10.1016/S1474-6670(17)50763-6)
- [26] A. D. Mammadov, E. Dincel, and M. T. Söylemez, “Analytical design of discrete pi-pr controllers via dominant pole assignment,” *ISA Transactions*, vol. 123, pp. 312–322, 2022. [Online]. Available: <https://doi.org/10.1016/j.isatra.2021.05.038>
- [27] P. Teppa-Garrán and J. Andrade-Da Silva, “An analytical interpolation approach for gain scheduling control of linear parameter varying systems,” *Ciencia e Ingeniería*, vol. 30, no. 1, pp. 93–101, 2008. [Online]. Available: <https://upsalesiana.ec/ing33ar2r27>
- [28] W. Tan, A. Packard, and G. Balas, “Quasi-lpv modeling and lpv control of a generic missile,” in *Proceedings of the 2000 American Control Conference. ACC (IEEE Cat. No.00CH36334)*, vol. 5, 2000, pp. 3692–3696. [Online]. Available: <https://doi.org/10.1109/ACC.2000.879259>
- [29] G. Vinco, S. Theodoulis, O. Sename, and G. Strub, “Quasi-lpv modeling of guided projectile pitch dynamics through state transformation technique,” *IFAC-PapersOnLine*, vol. 55, no. 35, pp. 43–48, 2022, 5th IFAC Workshop on Linear Parameter Varying Systems LPVS 2022. [Online]. Available: <https://doi.org/10.1016/j.ifacol.2022.11.288>
- [30] Z. He and L. Zhao, “Quadrotor trajectory tracking based on quasi-lpv system and internal model control,” *Mathematical Problems in Engineering*, vol. 2015, no. 1, p. 857291, 2015. [Online]. Available: <https://doi.org/10.1155/2015/857291>
- [31] P. S. Cisneros, A. Sridharan, and H. Werner, “Constrained predictive control of a robotic manipulator using quasi-lpv representations,” *IFAC-PapersOnLine*, vol. 51, no. 26, pp. 118–123, 2018, 2nd IFAC Workshop on Linear Parameter Varying Systems LPVS 2018. [Online]. Available: <https://doi.org/10.1016/j.ifacol.2018.11.158>
- [32] H. Xie, L. Dai, Y. Lu, and Y. Xia, “Disturbance rejection mpc framework for input-affine nonlinear systems,” *IEEE Transactions on Automatic Control*, vol. 67, no. 12, pp. 6595–6610, 2022. [Online]. Available: <https://doi.org/10.1109/TAC.2021.3133376>
- [33] J. Stefanovski, “Feedback affinization of nonlinear control systems,” *Systems & Control Letters*, vol. 46, no. 3, pp. 207–217, 2002. [Online]. Available: [https://doi.org/10.1016/S0167-6911\(02\)00136-6](https://doi.org/10.1016/S0167-6911(02)00136-6)
- [34] J. Apkarian, *Coupled water tank experiments manual*. Quanser Consulting Advanced Teaching Systems, 1999. [Online]. Available: <https://upsalesiana.ec/ing33ar2r34>
- [35] R. C. Dorf and R. H. Bishop, *Modern Control Systems*. Prentice Hall, 2008. [Online]. Available: <https://upsalesiana.ec/ing33ar2r35>
- [36] A. Bartlett, C. Hollot, and H. Lin, “Root locations of an entire polytope of polynomials: It suffices to check the edges,” in *1987 American Control Conference*, 1987, pp. 1611–1616. [Online]. Available: <https://doi.org/10.23919/ACC.1987.4789571>